The use of rapid small-scale column tests to determine the efficiency of bauxite residue as a low-cost adsorbent in the removal of dissolved reactive phosphorus from agricultural waters.

Patricia B. Cusack[a,b,c], Oisín Callery[d], Ronan Courtney[a,c], Éva Ujaczki[c,e,f] Lisa M. T. O' Donoghue[f], Mark G. Healy[b*]

[a]Department of Biological Sciences, University of Limerick, Castletroy, Co. Limerick, Ireland.

[b]Civil Engineering, National University of Ireland, Galway, Ireland.

[c]The Bernal Institute, University of Limerick, Castletroy, Co. Limerick, Ireland.

[d]Earth and Ocean Sciences, National University of Ireland, Galway, Ireland.

[e]Department of Applied Biotechnology and Food Science, Faculty of Chemical Technology and Biotechnology, Budapest University of Technology and Economics, Műegyetem rkp. 3, 1111 Budapest, Hungary.

[f]School of Engineering, University of Limerick, Castletroy, Co. Limerick, Ireland.

*Corresponding Author. Tel: +353 91 495364; fax: +353 91 494507. Postal address: Alice Perry Engineering Building, College of Engineering and Informatics, National University of Ireland, Galway, Co. Galway, H91 HX31. E-mail address: mark.healy@nuigalway.ie

Highlights

- Bauxite residue was examined as an adsorbent for phosphorus using a column study.
- The bauxite residue had a service time of 1.08 min g^{-1} media for the forest run-off.
- The service time was 0.28 min g^{-1} media when treating dairy soiled water.
- The bauxite residue was examined before and after the adsorption process.

Abstract

Bauxite residue, the by-product produced in the alumina industry, is a potential low-cost adsorbent in the removal of phosphorus (P) from aqueous solution, due to its high composition of residual iron oxides such as hematite. Several studies have investigated the performance of bauxite residue in removing P; however, the majority have involved the use of laboratory "batch" tests, which may not accurately estimate its actual performance in filter systems. This study investigated the use of rapid small-scale column tests to predict the dissolved reactive phosphorus (DRP) removal capacity of bauxite residue when treating two agricultural waters of low (forest run-off) and high (dairy soiled water) phosphorus content. Bauxite residue was successful in the removal of DRP from both waters, but was more efficient in treating the forest run-off. The estimated service time of the column media, based on the largest column studied, was 1.08 min g^{-1} media for the forest run-off and 0.28 min g^{-1} media for the dairy soiled water, before initial breakthrough time, which was taken to be when the column effluent reached approximately 5% of the influent concentration, occurred. Metal(loid) leaching from the bauxite residue, examined using ICP-OES, indicated that aluminium and iron were the dominant metals present in the treated effluent, both of which were above the EPA parametric values (0.2 mg L^{-1} for both Al and Fe) for drinking water.

Keywords: bauxite residue; adsorbent; phosphorus; agricultural wastewater

Nomenclature

A	constant of proportionality (mg g^{-1})
a^{**}	a time constant.
Al	aluminium
Al_2O_3	aluminium oxide
As	arsenic
B	constant of system heterogeneity in Eqn. (1 and 2)
BRDA	bauxite residue disposal area
Ca	calcium
Cd	cadmium
C_t	solution adsorbate concentration at any filter depth (mg L^{-1})
C_o	influent contaminant concentration (mg L^{-1})
Cr	chromium
CRM	critical raw material
Cu	copper
DRP	dissolved reactive phosphorus (mg L^{-1})
DSW	dairy soiled water
EDS	energy-dispersive X-ray spectroscopy
Fe	iron
Fe_2O_3	iron oxide
Fl	fluoride
FT-IR	Fourier transform infrared
Ga	gallium
Hg	mercury

76	HNO_3	nitric acid
77	ICP-OES	inductively coupled plasma optical emission spectrometer
78	M	mass of filter media contained in the filter column (g)
79	Mg	magnesium
80	Mn	manganese
81	Mo	molybdenum
82	n	the number of containers in which the total volume of effluent is collected
83	N	nitrogen
84	Na	sodium
85	Ni	nickel
86	P	phosphorus
87	Pb	lead
88	pH	pH unit
89	q_e	cumulative mass of contaminant adsorbed per g of filter media (mg g^{-1})
90	q_t	time dependent sorbate concentration per unit mass of adsorbent (mg g^{-1}),
91	RSSCT	rapid small-scale column test
92	Se	selenium
93	SEM	scanning electron microscopy
94	t	Empty bed contact time of the column filter bed (min)
95	V	volume of the influent loaded onto the filter (L)
96	V	vanadium
97	V_B	number of empty bed volumes of influent/solution filtered
98	XRD	x-ray diffraction
99	XRF	x-ray fluorescence
100	Zn	zinc

1. Introduction

Phosphorus (P) is an essential component of all plant and animal life (Weissert and Kehr, 2018), and is critical in the production and maintenance of food supply (Cordell and White 2011; Pretty and Bharucha, 2014). Phosphorus is also identified as one of the key nutrients that leads to the eutrophication of water bodies, in which there is an excess production of algal blooms, resulting in detrimental effects to aquatic life (Pan *et al.,* 2018). Agricultural practices, such as the application of slurry and fertiliser, may result in the transport of nutrients in surface runoff (Murnane *et al.,* 2016; Pan *et al.,* 2018) and subsurface flow (O' Flynn *et al.,* 2018; Zhou *et al.,* 2016) to a water body, and have been identified as a major cause of eutrophication (Sharpley, 2016).

The movement of P from soil to water bodies is predominantly in the form of particulate or dissolved reactive P (DRP) (Brennan *et al.,* 2014), the latter being 100% available for aquatic biota and which, therefore, has an immediate effect on the surrounding ecosystems (Penn *et al.,* 2014). Conventional methods of P removal from water have involved the use of enhanced biological removal systems such as polyphosphate accumulating organisms (PAOs) (Ge *et al.,* 2015) and algal biofilms (Sukačová *et al.,* 2015), precipitation methods using hydrous ferric oxides (Hauduc *et al.,* 2015) or struvite (Zhou *et al.,* 2015), the use of adsorbents (Grace *et al.,* 2015; Callery *et al.,* 2016; Callery and Healy, 2017), ion exchange (Acelas *et al.,* 2015), and reverse osmosis (Wang *et al.,* 2016). In recent years, to address the concept of a 'circular economy' (United Nations, 2015), emphasis has been placed on the utilisation of industrial wastes as low-cost adsorbents (De Gisi *et al.,* 2016; Grace *et al.,* 2016). Materials that have been utilised include fly ash (Nowak *et al.,* 2013), steel slags (Claveau-Mallet *et al.,* 2013) and chemical amendments (Callery *et al.,* 2015). Particular

126 focus has been placed on bauxite residue (red mud), the by-product generated in the Bayer
127 Process during the extraction of alumina, as a potential low-cost P adsorbent in aqueous
128 solutions. It is currently being produced at a global rate of 150 Mt per annum (Evans 2016),
129 but only approximately 2 % of the bauxite residue produced is currently re-used (Ujaczki *et*
130 *al.,* 2018), with the remaining ~ 98% being disposed of into bauxite residue disposal areas
131 (BRDAs) (Burke *et al.,* 2013; Kong *et al.,* 2017). The general composition of bauxite residue
132 comprises high amounts of iron (Fe) and aluminium (Al) oxides (Zhu *et al.,* 2016), which are
133 good adsorbents of P. In addition, bauxite residue has a high specific surface area (Gräfe *et*
134 *al.,* 2011) and therefore has numerous potential adsorption sites, giving it increased capacity
135 for P retention. Previous laboratory studies have shown that bauxite residue has high P
136 adsorption capacity (Table 1).
137
138 Traditionally, bench-scale "batch" studies are conducted to evaluate the effectiveness of a
139 material to adsorb P (Table 1). These studies involve placing the material in small containers,
140 overlaying it with solutions of known concentrations, mixing for a period usually of between
141 24 to 48 hr, and then fitting the results obtained to an adsorption isotherm such as the
142 Freundlich or Langmuir, in order to quantify its adsorption potential (Cusack *et al.,* 2018;
143 Grace *et al.,* 2015). However, batch studies have some disadvantages, such as failing to
144 replicate the often passive nature of the adsorption process which exists on site, as well as
145 sometimes using unrealistic ratios of adsorbent to solution, and shaking of the samples
146 (ÁdÁm *et al.,* 2007; Søvik and Kløve, 2005). In addition, concerns have been raised about
147 their accuracy in replicating the actual performance when the adsorbent material is placed in
148 a filter and operated on site (Fenton *et al.,* 2009). Due to the nature of the batch experiment,
149 they also fail to realistically replicate any incidental releases of contaminants, which may
150 occur when some materials are placed in filters. This may be particularly pertinent in the

evaluation of the feasibility of bauxite residue, which contains metals (Cusack *et al.,* 2018). In order to determine the full potential and longevity of an adsorbent, larger scale "column" studies are necessary (Pratt *et al.,* 2012). In these studies, the material is placed in a column, usually operated at laboratory-scale, and water of a known concentration is passed through the material until the effluent concentration is the same as the influent concentration. These continuous flow column studies require vast amounts of influent water, which depending on the type of water utilised, is often difficult to source in the laboratory (Callery and Healy, 2017). On account of this, rapid, small-scale column studies which utilise smaller volumes of media and wastewater have been gaining in popularity, and have been used to successfully model the adsorbancies of P (Callery *et al.,* 2016; Lalley *et al.,* 2015), fluoride (Wu *et al.,* 2018), paracetamol (García-Mateos *et al.,* 2015), and varying species of arsenic (Tresintsi *et al.,* 2014).

As P adsorption tests on bauxite residues have been commonly conducted using batch-scale studies, which may have many shortcomings as detailed above, the objectives of this study were to use rapid, small-scale column studies to (1) to assess the potential of bauxite residue as a low-cost adsorbent for DRP removal from two types of agricultural waters (dairy soiled water (DSW) and forest run-off) (2) compare the composition of the bauxite residue before and after use in the column tests (3) investigate the speciation of P adsorption onto the bauxite residue, and (4) identify any potential trace metal mobilisation from the bauxite residue during the study.

2. Materials and Methods

2.1 Sample collection

Bauxite residue was obtained from a European refinery. Residue was sampled to a depth of 30 cm below the surface of the BRDA, returned to the laboratory and dried at 105˚C for 24 hr. Once dry, the samples were pulverised using a mortar and pestle and sieved to a particle size < 0.5 mm. The pH and electrical conductivity (EC) were measured (n=3) using 5 g of sample in an aqueous extract, using a 1:5 ratio (solid:liquid) (Courtney and Harrington, 2010). Dairy soiled water (milk parlour washings composed of cow faeces and urine, milk and detergents; Minogue *et al.,* 2015) was collected from Teagasc Agricultural Research Centre, Moorepark, Co. Cork, Ireland [52° 9’ 48.114” N, 8° 15’ 34.6464” W] and forest run-off was collected from Kilmoon, Co. Clare, Ireland [53° 2’ 48.0372” N, 9° 16’ 21.1368” W]. The DSW and forest run-off were transferred directly to a temperature-controlled room (11°C) prior to commencement of testing. The DRP was measured using filtered (0.45 µm) subsamples using a nutrient analyser (Konelab20, Thermo Clinical Lab systems, Finland) and the pH was measured using a Eutech Instruments pH 700 (Thermo Scientific, USA).

2.1.1 Media characterisation

The bauxite residue was characterised before and after the experiment. Mineralogical detection was carried out on 1 g powdered samples using X-ray diffraction (XRD) on a Philips X’Pert PRO MPD® (California, USA) at 40 kV, 40 mA, 25 °C by Cu X-ray tube (Kα-radiation). The patterns were collected in the angular range from 5 to 80 º (2ɵ) with a step-size of 0.008 º (2ɵ) (Castaldi *et al.,* 2011). The surface morphology and elemental detection were carried out using scanning electron microscopy (SEM) and energy-dispersive X-ray spectroscopy (EDS) on a Hitachi SU-70 (Berkshire, UK). X-ray fluorescence (XRF) analysis was carried out onsite at the refinery using a Panalytical Axios XRF.

2.2 Rapid Small Scale Column Study

Small bore adsorption columns were prepared after Callery *et al.* (2016) using polycarbonate tubes, with an internal diameter of 0.94 cm and lengths of 20, 30 and 40 cm. The tubes were packed with a mixture of bauxite residue. The bauxite residue was held in place within each column using acid-washed glass wool and plastic syringes with an internal diameter equal to outside diameter of the polycarbonate tube, placed at the top and bottom of each of the polycarbonate tube columns. To each end of the polycarbonate tube column, flexible silicone tubing was attached to the syringe ends in order to provide lines for the influent and effluent. The columns were secured on a metal frame, allowing for a stable, vertical orientation to be maintained. A Masterflex® L/S Variable-Speed Drive peristaltic pump (Gelsenkirchen, Germany) with a variable speed motor was used to pump the influent, DSW and forest run-off, into the base of each column at an estimated flow rate of 30.49 ± 0.85 mL hr^{-1} (equivalent to a hydraulic loading rate used in a P removal system for wastewater treatment on a poultry farm; Penn *et al.,* 2014). The pump was operated in 12 hr on/off cycles (to allow the filter media to replenish some of its adsorption sites) to achieve loading periods of 24 – 36 hr, in order to obtain enough data points for the determination of the adsorption model coefficients. Every 2 hr, aliquots of the filtered effluent were collected using an auto-sampler and measured for volume, pH and DRP.

The adsorption performance of the media was evaluated using a model developed by Callery and Healy (2017), wherein the column effluent (C_e) is taken as a function of the volume of influent treated (V) and breakthrough concentrations (BTCs) formed by plotting V (x-axis) against C_e (y-axis). The breakthrough of the column media was taken to be when the column effluent was approximately 5% of the influent concentration (Chen *et al.,* 2003). This model, which has been successful in the prediction of the performance of a large-scale filter (Callery

et al., 2016), was used in the prediction of the longevity of the bauxite residue in the current study.

The overall bauxite residue service time or longevity of the bauxite residue media can be found by first determining the volume treated, using Eqn. 1, where q_t is the time dependent sorbate concentration per unit mass of adsorbent (mg g^{-1}), M is the mass of the adsorbent (g), B is a constant of system heterogeneity, C_o is the sorbate concentration of the influent (mg L^{-1}) and C_t is the solution adsorbate concentration at any filter depth (mg L^{-1}), by dividing the volume treated, V (in L) by the loading rate (L s^{-1}) and then converting to minutes per g of media.

$$V = \frac{q_t M}{B\,(C_o - C_t)} \tag{1}$$

The q_t used in Eqn. 1 was calculated using Eqn. 2:

$$q_t = A V_B^{\left(\frac{1}{B}\right)} \left| \frac{t}{t + a^{**}} \right. \tag{2}$$

Where A is a constant of proportionality (mg L^{-1}), t is the empty bed contact time of the column filter bed (min), V_B is the number of empty bed volumes of influent/solution filtered, and a^{**} is a time constant.

2.3 Speciation of P adsorbed

Fourier transform infrared (FT-IR) analysis was carried out using a Perkin Elmer Spectrum 100 (PerkinElmer, USA). The FT-IR spectra were recorded in the 4000 to 650 cm^{-1} range and were collected after 256 scans at 4 cm^{-1} resolution (Castaldi *et al.,* 2010).

2.4 Trace metal analysis

Every 2 hr, 10 mL of the aliquot collected from the columns, was preserved in nitric acid (HNO_3), to a pH <2 and refrigerated before elemental analysis was carried out using an Agilent Technologies 5100 Inductively Coupled Plasma Optical Emission Spectrometer (ICP-OES). In order to carry out the ICP-OES analysis, a calibration curve was created using standardised solutions comprised of 100, 50, 10, 5 and 1 g L^{-1} multi element standard (Inorganic Ventures, Ireland) and 1M HNO_3. The analytical lines (in nm) used for the calculations of each element were as follows: Al 237.312, 396.152; calcium (Ca) 396.847, 422.673; cadmium (Cd) 214.439, 226.502, 228.802; chromium (Cr) 205.560, 267.716, 357.868; copper (Cu) 213.598, 324.754, 327.395; Fe 234.350, 238.204, 259.940; gallium (Ga) 287.423, 294.363, 417.204; mercury (Hg) 184.887, 194.164; magnesium (Mg) 279.553, 280.270, 285.213; manganese (Mn) 257.610, 259.372, 260.568; molybdenum (Mo) 202.032, 203.846, 204.598; sodium (Na) 589.592; nickel (Ni) 216.555, 221.648, 231.604; lead (Pb) 220.353, 283.305; selenium (Se) 196.026, 203.985; silicon (Si) 250.690, 251.611, 288.158; vanadium (V) 268.796, 292.401, 309.310; zinc (Zn) 202.548, 206.200, 213.857 (Bridger and Knowles, 2010). The XRF analysis performed on the bauxite residue was carried out using a Panalytical Axios XRF (Malvern Panalytical Ltd., United Kingdom).

3. Results and Discussion

3.1 Media characterisation before and after the experiments

Bauxite residue typically comprises Fe, Al, Ti, Si, Na and Ca, mainly in the form of oxides (Gräfe et *al.*, 2011). The presence of Fe and Al oxides, which can range from 5 to 60 and 5 to 30 %, respectively (Evans, 2016), and Ti oxides, which are typically in the range of 0.3 to 15 % (Evans, 2016), mean that bauxite residue is a potential adsorbent for both cations and

anions from aqueous solutions (Bhatnagar *et al.,* 2011; Cusack *et al.,* 2018). This is why numerous studies have investigated the potential of P removal from aqueous solution (Table 1).

The main mineralogical composition of the bauxite residue used in this study comprised mainly iron and aluminium oxides (Fe_2O and Al_2O_3) (Table 2). SEM-EDS analysis also indicated the dominance of Fe and Al (Figure S1 in the Supplementary Information). Titanium, Si, Ca and Na were also detected in the main composition. Prior to use in the column, there was a mineralogical dominance of the iron oxide hematite (as represented by H in Figure 1), detected at positions 33.153 and 35.612°2Θ, respectively (Figure 1). Rutile (TiO_2) was also detected at position 27.459 °2Θ. Following the column trials, XRD analysis was carried out on the spent media from both the DSW and forest run-off columns. New peaks were identified in the XRD patterns, as seen in Figure 1, which show the presence of P-based minerals, which were not present in the raw media. The new peaks detected in both the spent media following treatment of the DSW and forest run-off was calcium hydrogenphosphate (III) hydrate ($CaHPO_4^{3-}$) at positions 19.120 and 30.001 °2Θ. The presence of this mineral in the spent media indicates P retention within the bauxite residue after treatment. The particle size analysis (PSA) of the bauxite residue used in this study is shown in Table 3.

3.2 Influent and effluent water characterisation and rapid small-scale column study

The forest run-off had a pH of 7.57 and a DRP concentration of 1.10 mg P L^{-1}. The total phosphorus (TP) concentration of forest run-off is usually around 1 mg L^{-1} (Finnegan *et al.,* 2012), whereas DSW has a TP concentration of 20 to 100 mg L^{-1} and a total nitrogen (TN)

300 concentration of 70 to 500 mg L^{-1} (Minogue *et al.*, 2015). The DSW used in this study had a
301 pH of 7.79 and a DRP concentration of 10.64 mg P L^{-1}.
302
303 The BTC approached saturation much quicker for the DSW than for the forest run-off water
304 (Figure 2). Similar to the findings of Vuković *et al.* (2011), the breakthrough time and
305 exhaustion time increased with bed depth. As a result of its composition, there are other
306 anions such as nitrates (NO_3^-) and nitrites (NO_2^-) present in the DSW (Ruane *et al.*, 2011),
307 and therefore there is greater competitiveness for available adsorption sites and interferences
308 between the adsorbent surface and the ions present in the aqueous solution. This may explain
309 why the DSW-treating columns generated a BTC approaching saturation much faster than the
310 bauxite residue columns treating forest run-off. When treating the forest run-off, the bauxite
311 residue had a service time of approximately 22.80 min, based on the largest column before
312 the initial breakthrough time of the bauxite residue occurred. However, when treating the
313 DSW, it had a shorter service time of 5.80 min, as noted for the largest column before the
314 initial breakthrough occurred. Taking into account the amount of bauxite residue used in the
315 largest columns (21.16 and 20.78 g), this gives an estimated service time of 1.08 min g^{-1}
316 bauxite residue and 0.28 min g^{-1} bauxite residue when treating forest run-off and DSW,
317 respectively, before initial breakthrough (5%) would occur.
318
319 The modelled q_t value for the bauxite residue was 0.27 mg P g^{-1} media and 0.045 mg P g^{-1}
320 media for the DSW and forest run-off, respectively. This is a lower value than that recorded
321 by Despland *et al.* (2011), who reported values of between 2.85 and 8.74 mg P g^{-1} of Bauxsol
322 (neutralised bauxite residue using synthetic brine water based on a seawater neutralisation
323 technique) media used. Although the values reported in this study are lower, it is important
324 to note that full saturation of the bauxite residue was not reached.

325

326 3.3 Speciation of P adsorbed

327 The adsorption of phosphate ions onto an adsorbent is measured by the decrease for
328 phosphate in the influent after a certain amount of time (Loganathan *et al.,* 2014). Typically,
329 the main mechanism of phosphate adsorption (and other anions and cations) onto the surface
330 of iron and aluminium oxides may be separated into two processes: specific and non-specific
331 adsorption (Stumm, 1992; Cornell and Schwertmann, 2003). Specific adsorption takes place
332 through the process of ligand exchange (Jacukowicz-Sobala *et al.,* 2015). A phosphate ion
333 exchanges with one or more hydroxyl groups, with the release of OH_2 and/or OH^- back into
334 the surrounding solution, contributing to the alkalisation of the surrounding environment
335 (Cornell and Schwertmann, 2003), as shown in the following equations:

336

337 $$\equiv \mathrm{FeOH} + \mathrm{An}^- \leftrightarrow \equiv \mathrm{FeAn} + \mathrm{OH}^- \quad (3)$$

338 $$\equiv \mathrm{Fe(OH)_2} + \mathrm{An}^- \leftrightarrow \equiv \mathrm{Fe_2} + \mathrm{An}^+ + 2\mathrm{OH}^- \quad (4)$$

339

340 Non-specific adsorption, which was the main mechanism evident in this study, is inclusive of
341 electrostatic interactions and surface precipitation (Loganathan *et al.,* 2014) between the
342 surface of the sorbent and the phosphate ion (Jacukowicz-Sobala *et al.,* 2015). The
343 electrostatic interactions occur between the electric charge carried on the surface of the
344 sorbent and type of ion present in the surrounding solution. Phosphate ions, which are of
345 anionic nature, carry a negative charge, which interacts with the positive charge as carried by
346 Ca, a cation (Loganathan *et al.,* 2014). Surface precipitation involves the formation of
347 complexes/precipitates on the surface of the sorbent such as $CaHPO_4^{3-}$ as a result of these ion
348 interactions (Loganathan *et al.,* 2014). The adsorption of the phosphate ions is greatest in a

low pH environment due to the abundance of positively charged sites (Jacukowicz-Sobala *et al.,* 2015).

X-ray diffraction and SEM analysis have been used in previous studies to show evidence of the presence of newly formed surface precipitates following the P adsorption process (Bowden et al., 2009). The XRD data obtained in this study (Figure 1) show that the main interactions and complexes formed by the phosphate ions present in the wastewater (negative charge) were with Ca (positive charge) present in the bauxite residue, as evidenced by the presence of new peaks of $CaHPO_4^{3-}$ in the XRD patterns following the treatment of both the DSW and forest run-off.. Depending on the pH of the solution, the species of P found in aqueous solution are H_3PO_4 (pH < 4), $H_2PO_4^-$ (pH ~ 0-9), HPO_4^{2-} (pH ~ 5-11) and PO_4^{3-} (pH >10) (Karageorgiou *et al.,* 2007; Despland *et al.,* 2011).

The FT-IR analysis of the bauxite residue media before and after treatment of both the DSW and forest run-off (Figures 3 and 4) indicated that similar changes occurred in the media following treatment of both wastewaters. Two distinct broad bands were detected between wavelength 600 to 900 cm^{-1} and again at 1000 to 1400 cm^{-1}. This was evident for both the DSW and forest run-off spent media. Intensive IR absorption bands are typically in the range of 560 to 600 cm^{-1} and 1000 to 1100 cm^{-1} for P species (Tejedor-Tejedor and Anderson, 1990; Berzina-Cimdina and Borodajenko, 2012). However, it was not possible to identify specific P species due to some interferences, which are most likely due to the presence of many other ions present in each of the wastewater sources used.

There was an increase in the pH in the effluent for both the DSW and forest run-off treated wastewater (Figure 5). The influent pH of the DSW was 7.79, which increased to 8.94 in the

374 40 cm column at t = 2 hr. The influent pH of the forest run-off was 7.57 and increased to 8.81
375 at t = 12 hr in the 40 cm column. According to the Drinking Water Directive (98/83/EC), the
376 pH value should be in the range of ≥ 6.5 and ≤ 9.5. The values recorded in this study show
377 that the pH values in the effluent are within this range, highlighting no potential risk to the
378 surrounding environment.
379
380 3.4 Trace metal and elemental analysis
381 Due to the complex nature of bauxite residue and its composition, there is potential for trace
382 metal leaching to the surrounding environment (Despland *et al.*, 2011; Evans, 2016).
383 Pollution from metals can have an adverse and detrimental effect on the surrounding
384 environment, affecting plant and animal life (Gomes *et al.*, 2016a; Olszewska *et al.*, 2017). In
385 addition, the majority of metals that are in a soil environment are non-degradable (Guo *et al.*,
386 2006).
387
388 The influent and effluent metal concentrations from the columns treating DSW and forest
389 run-off, along with the parametric values, as mandated by the Irish EPA (2014), are displayed
390 in Figures 6 and 7. In this study, the dominant species present in both effluents were Al and
391 Fe, which were above the parametric values (0.2 mg L^{-1} for both Al and Fe). Copper was
392 released in both effluents, but did decrease with loading time when treating the DSW and the
393 level of Cu reduced to below the parametric value of 2 mg L^{-1}. The level of Mn was lower in
394 the effluent compared to the influent for all columns, showing a retention capacity within the
395 column media, but it was higher than the parametric value of 0.05 mg L^{-1}. Magnesium, Ga,
396 V and Zn were also present in increased amounts in the effluent, due to leaching from the
397 bauxite residue. However, the Mg and Zn did decrease with increasing loading time. There
398 are currently no parametric values or EPA guideline values for drinking water parameters for

399 Mg, Ga, V and Zn, although previous studies have highlighted that bauxite residue is
400 inclusive of oxyanionic-forming elements, which are soluble at high pH range; these include
401 Al, As, Cr, Mo and V (Mayes *et al.,* 2016). The main species of V present in bauxite residue
402 was in the pentavalent form (Burke *et al.,* 2012, 2013), which may be problematic due to its
403 toxicity (Burke *et al.*, 2012). Whilst V may be a potential issue (depending on the source of
404 bauxite ore), it is also the focus of critical raw material (CRM) recovery studies (Gomes *et*
405 *al.,* 2016b; Zhu *et al.,* 2018), which suggests the potential and need for further studies
406 investigating the adsorbent potential of bauxite residue following the removal and recovery of
407 CRMs such as V.
408
409 Previous work by Lopez et al. (1998) highlighted the ability of bauxite residue to retain Ni,
410 Cu and Zn. Despland *et al.* (2014) showed that Bauxsol™ (neutralised bauxite residue
411 produced using the Basecon™ procedure) had the ability to remove trace amounts of As, lead
412 (Pb), Cd, Cr, Cu, Ni, Se, Zn, Mn and Al. This highlights the potential of bauxite residue in
413 the removal of both cations and anions from aqueous solution. However, the composition and
414 concentration of elements in bauxite will vary depending on the type of ore (Mayes *et al.,*
415 2011).
416
417 Although there was overall evidence of mobilisation of some trace elements while treating
418 the wastewater, one suggestion would be to include a rinse/wash period prior to packing the
419 columns. This would reduce and/or eliminate the potential leaching of metals at the initial
420 loading period and avoid further release as the loading period increases. Another option
421 would be to apply a seawater treatment to the bauxite residue, which has been proven to
422 lower the pH and therefore reduce the leaching of metal(loid) species (Cusack *et al.,* 2018;
423 Johnston *et al.,* 2010).

4. Conclusions

Several studies have focussed on the use of low-cost adsorbents in the removal of contaminants such as P from contaminated waters due to possible cost savings and to reutilise by-products from various sectors. This study demonstrated that bauxite residue has P (particularly dissolved reactive phosphorus) removal capabilities in both low (forest run-off) and high (dairy soiled water) range P-concentrated waters. The estimated service time of the column media before initial breakthrough, based on the performance of the largest columns, was 1.08 min g^{-1} media for the forest run-off and 0.28 min g^{-1} media for the dairy soiled water. Due to the composition of the bauxite residue, potential for metal(loid) leaching is a concern. Aluminium and iron were the dominant metals released in the treated effluent, but this may be eliminated by a preventative step such as introducing a washing period or a seawater neutralisation step prior to packing the bauxite residue into the columns.

Acknowledgements

The authors would like to acknowledge the financial support of the Environmental Protection Agency (EPA) (2014-RE-MS-1).

References

Acelas, N.Y., Martin, B.D., López, D. and Jefferson, B., 2015. Selective removal of phosphate from wastewater using hydrated metal oxides dispersed within anionic exchange media. *Chemosphere 119*, 1353-1360. DOI Link: https://doi.org/10.1016/j.chemosphere.2014.02.024

ÁdÁm, K., Sovik, A.K., Krogstad, T. and Heistad, A., 2007. Phosphorous removal by the filter materials light-weight aggregates and shellsand-a review of processes and experimental set-ups for improved design of filter systems for wastewater treatment. *Vatten 63*(3), 245.

Akhurst, D.J., Jones, G.B., Clark, M. and McConchie, D., 2006. Phosphate removal from aqueous solutions using neutralised bauxite refinery residues (Bauxsol™). *Environ. Chem. 3*(1), 65-74. DOI Link: https://doi.org/10.1071/EN05038

Berzina-Cimdina, L. and Borodajenko, N., 2012. Research of calcium phosphates using Fourier transform infrared spectroscopy. In *Infrared Spectroscopy-Materials Science, Engineering and Technology*. InTech. Available: http://scholar.google.com/scholar_url?url=https%3A%2F%2Fwww.intechopen.com%2Fdownload%2Fpdf%2F36171&hl=en&sa=T&oi=ggp&ct=res&cd=0&d=18760135324139934 55&ei=JQ5fW6ODB4SQmwHoq7O4BA&scisig=AAGBfm0zcrG1iAsbV5Fv1kKQs9aPk9QMNA&nossl=1&ws=1440x845 [accessed 30.07.2018].

Bhatnagar, A., Vilar, V.J., Botelho, C.M. and Boaventura, R.A., 2011. A review of the use of red mud as adsorbent for the removal of toxic pollutants from water and wastewater. Environ. Technol. 32(3), 231-249. DOI Link: https://doi.org/10.1080/09593330.2011.560615

Bowden, L.I., Jarvis, A.P., Younger, P.L. and Johnson, K.L., 2009. Phosphorus removal from waste waters using basic oxygen steel slag. Environmental science & technology, 43(7), pp.2476-2481.

Brennan, R.B., Wall, D., Fenton, O., Grant, J., Sharpley, A.N. and Healy, M.G., 2014. The impact of chemical amendment of dairy cattle slurry before land application on soil phosphorus dynamics. *Commun. Soil Sci. Plant Anal.* 45(16), 2215 – 2233. DOI Link: http://dx.doi.org/10.1080/00103624.2014.912293

Bridger, S. and Knowles, M., 2000. A complete method for environmental samples by simultaneous axially viewed ICP-AES following USEPA guidelines. Varian ICP-OES At Work (29) Available: https://www.agilent.com/cs/library/applications/ICPES-29.pdf [24.05.2018].

Burke, I.T., Mayes, W.M., Peacock, C.L., Brown, A.P., Jarvis, A.P. and Gruiz, K., 2012. Speciation of arsenic, chromium, and vanadium in red mud samples from the Ajka spill site, Hungary. *Environ. Sci. Technol. 46*(6), 3085-3092. DOI Link: 10.1021/es3003475

Burke, I.T., Peacock, C.L., Lockwood, C.L., Stewart, D.I., Mortimer, R.J., Ward, M.B., Renforth, P., Gruiz, K. and Mayes, W.M., 2013. Behavior of aluminum, arsenic, and

vanadium during the neutralization of red mud leachate by HCl, gypsum, or seawater. *Environ. Sci.Technol.* 47(12), 6527-6535. DOI Link: 10.1021/es4010834

Callery, O., Brennan, R.B. and Healy, M.G., 2015. Use of amendments in a peat soil to reduce phosphorus losses from forestry operations. *Ecol. Eng.* 85, 193 – 200. DOI Link: https://doi.org/10.1016/j.ecoleng.2015.10.016

Callery, O., Healy, M.G., Rognard, F., Barthelemy, L. and Brennan, R.B., 2016. Evaluating the long-term performance of low-cost adsorbents using small-scale adsorption column experiments. *Water Res. 101*, 429-440. DOI Link: https://doi.org/10.1016/j.watres.2016.05.093

Callery, O. and Healy, M.G., 2017. Predicting the propagation of concentration and saturation fronts in fixed-bed filters. *Water Res. 123*, 556-568. DOI Link: https://doi.org/10.1016/j.watres.2017.07.010

Castaldi, P., Silvetti, M., Enzo, S. and Melis, P., 2010. Study of sorption processes and FT-IR analysis of arsenate sorbed onto red muds (a bauxite ore processing waste). *J. Hazard. Mater.* *175*(1-3), 172-178. DOI Link: https://doi.org/10.1016/j.jhazmat.2009.09.145

Castaldi, P., Silvetti, M., Enzo, S. and Deiana, S., 2011. X-ray diffraction and thermal analysis of bauxite ore-processing waste (red mud) exchanged with arsenate and phosphate. *Clays Clay Miner.* 59(2), 189-199. DOI Link: https://doi.org/10.1346/CCMN.2011.0590207

Chen, J.P., Yoon, J.T. and Yiacoumi, S., 2003. Effects of chemical and physical properties of influent on copper sorption onto activated carbon fixed-bed columns. *Carbon* 41(8), 1635-1644. DOI Link: https://doi.org/10.1016/S0008-6223(03)00117-9

Claveau-Mallet, D., Wallace, S. and Comeau, Y., 2013. Removal of phosphorus, fluoride and metals from a gypsum mining leachate using steel slag filters. *Water Res. 47*(4), 1512-1520. DOI Link: https://doi.org/10.1016/j.watres.2012.11.048

Cordell, D. and White, S., 2011. Peak phosphorus: clarifying the key issues of a vigorous debate about long-term phosphorus security. *Sustainability 3*(10), 2027-2049. DOI Link: https://doi.org/10.3390/su3102027

Cornell, R.M. and Schwertmann, U., 2003. *The iron oxides: structure, properties, reactions, occurrences and uses*. John Wiley & Sons. Available: https://books.google.ie/books?hl=en&lr=&id=dlMuE3_klW4C&oi=fnd&pg=PA1&dq=Cornell,+R.M.+and+Schwertmann,+U.,+2003.+The+iron+oxides:+structure,+properties,+reactions,+occurrences+and+uses.+John+Wiley+%26+Sons.&ots=l0jQWg_4gN&sig=kNxeJyUHBF3-UemiW-s_EvlaeCs&redir_esc=y#v=onepage&q=Cornell%2C%20R.M.%20and%20Schwertmann%2C%20U.%2C%202003.%20The%20iron%20oxides%3A%20structure%2C%20properties%2C%20reactions%2C%20occurrences%20and%20uses.%20John%20Wiley%20%26%20Sons.&f=false [accessed 11.09.2018].

543 Courtney, R. and Harrington, T., 2010. Assessment of plant-available phosphorus in a fine
544 textured sodic substrate. *Ecol. Eng.* 36(4), 542-547. DOI Link:
545 https://doi.org/10.1016/j.ecoleng.2009.12.001
546
547 Cusack, P.B., Healy, M.G., Ryan, P.C., Burke, I.T., O'Donoghue, L.M., Ujaczki, É. and
548 Courtney, R., 2018. Enhancement of bauxite residue as a low-cost adsorbent for phosphorus
549 in aqueous solution, using seawater and gypsum treatments. *J. Clean Prod. 179*, 217-224.
550 DOI Link: https://doi.org/10.1016/j.jclepro.2018.01.092
551
552 De Gisi, S., Lofrano, G., Grassi, M. and Notarnicola, M., 2016. Characteristics and
553 adsorption capacities of low-cost sorbents for wastewater treatment: a review. *Sustainable*
554 *Mater. Technol. 9*, 10-40. DOI Link: https://doi.org/10.1016/j.susmat.2016.06.002
555
556 Despland, L.M., Clark, M.W., Vancov, T., Erler, D. and Aragno, M., 2011. Nutrient and
557 trace-metal removal by Bauxsol pellets in wastewater treatment. *Environ. Sci. Technol.*
558 *45*(13), 5746-5753. DOI Link: https://doi.org/10.1021/es200934y
559
560 Despland, L.M., Clark, M.W., Vancov, T. and Aragno, M., 2014. Nutrient removal and
561 microbial communities' development in a young unplanted constructed wetland using
562 Bauxsol™ pellets to treat wastewater. *Sci. Total Environ. 484*, 167-175. DOI Link:
563 https://doi.org/10.1016/j.scitotenv.2014.03.030
564
565 EPA, 2014. Drinking Water Parameters Microbiological, Chemical and Indicator Parameters
566 in the 2014 Drinking Water Regulations. Available:

www.epa.ie/pubs/advice/drinkingwater/2015_04_21_ParametersStandaloneDoc.pdf [accessed 29.05.2018].

European Drinking Water Directive (Council Directive 98/83/EC of 3 November 1998 on the quality of water intended for human consumption) (1998). Available: https://eur-lex.europa.eu/legal-content/EN/TXT/PDF/?uri=CELEX:31998L0083&from=EN [accessed 20.07.208].

Evans, K., 2016. The history, challenges, and new developments in the management and use of bauxite residue. *J. Sustainable Metallurgy* 2(4), 316-331. DOI Link: https://doi.org/10.1007/s40831-016-0060-x

Fenton, O., Healy, M.G., Rodgers, M. 2009. Use of ochre from an abandoned metal mine in the south east of Ireland for phosphorus sequestration from dairy dirty water. *J. Environ. Qual.* 38, 1120 – 1125. DOI Link: https://doi.org/10.2134/jeq2008.0227

Finnegan, J., Regan, J.T., De Eyto, E., Ryder, E., Tiernan, D. and Healy, M.G., 2012. Nutrient dynamics in a peatland forest riparian buffer zone and implications for the establishment of planted saplings. *Ecol. Eng. 47*, 155-164. DOI Link: https://doi.org/10.1016/j.ecoleng.2012.06.023

García-Mateos, F.J., Ruiz-Rosas, R., Marqués, M.D., Cotoruelo, L.M., Rodríguez-Mirasol, J. and Cordero, T., 2015. Removal of paracetamol on biomass-derived activated carbon: modeling the fixed bed breakthrough curves using batch adsorption experiments. *Chem. Eng. J. 279*, 18-30. DOI Link: https://doi.org/10.1016/j.cej.2015.04.144

Ge, H., Batstone, D.J. and Keller, J., 2015. Biological phosphorus removal from abattoir wastewater at very short sludge ages mediated by novel PAO clade Comamonadaceae. *Water Res. 69*, 173-182. DOI Link: https://doi.org/10.1016/j.watres.2014.11.026

Gomes, H.I., Mayes, W.M., Rogerson, M., Stewart, D.I. and Burke, I.T., 2016. Alkaline residues and the environment: a review of impacts, management practices and opportunities. *J. Clean Prod.* 112, 3571-3582. DOI Link: https://doi.org/10.1016/j.jclepro.2015.09.111

Gomes, H.I., Jones, A., Rogerson, M., Burke, I.T. and Mayes, W.M., 2016. Vanadium removal and recovery from bauxite residue leachates by ion exchange. *Environ. Sci. Poll. Res. 23*(22), 23034-23042. DOI Link: https://doi.org/10.1007/s11356-016-7514-3

Grace, M.A., Healy, M.G. and Clifford, E., 2015. Use of industrial by-products and natural media to adsorb nutrients, metals and organic carbon from drinking water. *Sci. Total Environ. 518*, 491-497. DOI Link: https://doi.org/10.1016/j.scitotenv.2015.02.075

Grace, M.A., Clifford, E. and Healy, M.G., 2016. The potential for the use of waste products from a variety of sectors in water treatment processes. *J. Clean Prod. 137*, 788-802. DOI Link: https://doi.org/10.1016/j.jclepro.2016.07.113

Gräfe, M., Power, G. and Klauber, C., 2011. Bauxite residue issues: III. Alkalinity and associated chemistry. *Hydrometallurgy, 108*(1-2), 60-79. DOI Link: https://doi.org/10.1016/j.hydromet.2011.02.004

Guo, G., Zhou, Q. and Ma, L.Q., 2006. Availability and assessment of fixing additives for the in situ remediation of heavy metal contaminated soils: a review. *Environ. Monit. Assess.* *116*(1-3), 513-528. DOI Link: https://doi.org/10.1007/s10661-006-7668-4

Hauduc, H., Takács, I., Smith, S., Szabo, A., Murthy, S., Daigger, G.T. and Spérandio, M., 2015. A dynamic physicochemical model for chemical phosphorus removal. *Water Res. 73*, 157-170. DOI Link: https://doi.org/10.1016/j.watres.2014.12.053

Herron, S.L., Sharpley, A.N., Brye, K.R. and Miller, D.M., 2016. Optimizing hydraulic and chemical properties of iron and aluminum byproducts for use in on-farm containment structures for phosphorus removal. *J. Environ. Protection 7*(12), 1835. DOI Link: https://doi.org/ 10.4236/jep.2016.712146

Huang, W., Wang, S., Zhu, Z., Li, L., Yao, X., Rudolph, V. and Haghseresht, F., 2008. Phosphate removal from wastewater using red mud. *J. Hazard. Mater. 158*(1), 35-42. DOI Link: https://doi.org/10.1016/j.jhazmat.2008.01.061

Jacukowicz-Sobala, I., Ociński, D. and Kociołek-Balawejder, E., 2015. Iron and aluminium oxides containing industrial wastes as adsorbents of heavy metals: application possibilities and limitations. *Waste Manage. Res. 33*(7), 612-629. DOI Link: https://doi.org/10.1177/0734242X15584841

Johnston, M., Clark, M.W., McMahon, P. and Ward, N., 2010. Alkalinity conversion of bauxite refinery residues by neutralization. *J. Hazard. Mater.* 182(1-3), 710-715. DOI Link: https://doi.org/10.1016/j.jhazmat.2010.06.091

642

643 Karageorgiou, K., Paschalis, M. and Anastassakis, G.N., 2007. Removal of phosphate species
644 from solution by adsorption onto calcite used as natural adsorbent. *J. Hazard. Mater. 139*(3),
645 447-452. DOI Link: https://doi.org/10.1016/j.jhazmat.2006.02.038

646

647 Kong, X., Li, M., Xue, S., Hartley, W., Chen, C., Wu, C., Li, X. and Li, Y., 2017. Acid
648 transformation of bauxite residue: conversion of its alkaline characteristics. *J. Hazard. Mater.*
649 *324*, 382-390. DOI Link: https://doi.org/10.1016/j.jhazmat.2016.10.073

650

651 Lalley, J., Han, C., Mohan, G.R., Dionysiou, D.D., Speth, T.F., Garland, J. and Nadagouda,
652 M.N., 2015. Phosphate removal using modified Bayoxide® E33 adsorption media. *Environ.*
653 *Sci. Water Res. Technol. 1*(1), 96-107. DOI Link: https://doi.org/10.1039/C4EW00020J

654

655 Liu, Y., Lin, C. and Wu, Y., 2007. Characterization of red mud derived from a combined
656 Bayer Process and bauxite calcination method. *J. Hazard. Mater.* 146, 255-261. DOI Link:
657 https://doi.org/10.1016/j.jhazmat.2006.12.015

658

659 Loganathan, P., Vigneswaran, S., Kandasamy, J. and Bolan, N.S., 2014. Removal and
660 recovery of phosphate from water using sorption. Critical Reviews in Environmental Science
661 and Technology, 44(8), pp.847-907.

662

663 Lopez, E., Soto, B., Arias, M., Nunez, A., Rubinos, D. and Barral, M.T., 1998. Adsorbent
664 properties of red mud and its use for wastewater treatment. *Water Res.* 32, 1314-1322. DOI
665 Link: https://doi.org/10.1016/S0043-1354(97)00326-6

666

667 Mayes, W.M., Jarvis, A.P., Burke, I.T., Walton, M., Feigl, V., Klebercz, O. and Gruiz, K.,
668 2011. Dispersal and attenuation of trace contaminants downstream of the Ajka bauxite
669 residue (red mud) depository failure, Hungary. *Environ. Sci. Technol. 45*(12), 5147-5155.
670 DOI Link: https://doi.org/ 10.1021/es200850y
671
672 Mayes, W.M., Burke, I.T., Gomes, H.I., Anton, Á.D., Molnár, M., Feigl, V. and Ujaczki, É.,
673 2016. Advances in understanding environmental risks of red mud after the Ajka spill,
674 Hungary. *J. Sustainable Metallurgy 2*(4), 332-343. DOI Link:
675 https://doi.org/10.1007/s40831-016-0050-z
676
677 McConchie, D., Clark, M., Davies-McConchie, F., 2001. Processes and Compositions for
678 Water Treatment, Neauveau Technology Investments, Australian, p. 28.
679
680 Minogue, D., French, P., Bolger, T. and Murphy, P.N.C., 2015. Characterisation of dairy
681 soiled water in a survey of 60 Irish dairy farms. *Irish J. Agricultural and Food Res. 54*(1), 1-
682 16. DOI Link: https://doi.org/10.1515/ijafr-2015-0001
683
684 Murnane, J.G., Brennan, R.B., Fenton, O. and Healy, M.G., 2016. Zeolite combined with
685 alum and aluminium chloride mixed with agricultural slurries reduces carbon losses in runoff
686 from grassed soil boxes. *J. Environ. Qual.* 44(5), 1674 – 1683. DOI Link:
687 https://doi.org/10.2134/jeq2016.05.0175
688
689 Nowak, B., Aschenbrenner, P. and Winter, F., 2013. Heavy metal removal from sewage
690 sludge ash waste fly ash—a comparison. *Fuel Process. Technol. 105*, 195-201. DOI Link:
691 https://doi.org/10.1016/j.fuproc.2011.06.027

692

693 O'Flynn, C.J., Fenton, O., Wall, D., Brennan, R.B., McLaughlin, M.J. and Healy, M.G.,
694 2018. Influence of soil phosphorus status, texture, pH and metal content on the efficacy of
695 amendments to pig slurry in reducing phosphorus losses. *Soil Use and Management 34*(1), 1-
696 8. DOI Link: https://doi.org/10.1111/sum.12391

697

698 Olszewska, J.P., Heal, K.V., Winfield, I.J., Eades, L.J. and Spears, B.M., 2017. Assessing the
699 role of bed sediments in the persistence of red mud pollution in a shallow lake (Kinghorn
700 Loch, UK). *Water Res.123*, 569-577. DOI Link: https://doi.org/10.1016/j.watres.2017.07.009

701

702 Pan, G., Lyu, T. and Mortimer, R., 2018. Comment: closing phosphorus cycle from natural
703 waters: re-capturing phosphorus through an integrated water-energy-food strategy. DOI
704 Link: https://doi.org/10.1016/j.jes.2018.02.018.

705

706 Penn, C., McGrath, J., Bowen, J. and Wilson, S., 2014. Phosphorus removal structures: A
707 management option for legacy phosphorus. *J. Soil Water Conserv. 69*(2), 51A-56A. DOI
708 Link: https://doi.org/10.2489/jswc.69.2.51A

709

710 Pratt, C., Parsons, S.A., Soares, A. and Martin, B.D., 2012. Biologically and chemically
711 mediated adsorption and precipitation of phosphorus from wastewater. *Curr. Opin.*
712 *Biotechnol. 23*(6), 890-896. DOI Link: https://doi.org/10.1016/j.copbio.2012.07.003

713

714 Pretty, J. and Bharucha, Z.P., 2014. Sustainable intensification in agricultural systems.
715 *Annals of Botany 114*(8), 1571-1596. DOI Link: https://doi.org/10.1093/aob/mcu205

716

717 Ruane, E.M., Murphy, P.N., Healy, M.G., French, P. and Rodgers, M., 2011. On-farm
718 treatment of dairy soiled water using aerobic woodchip filters. *Water Res. 45*(20), 6668-6676.
719 DOI Link: https://doi.org/10.1016/j.watres.2011.09.055
720
721 Sharpley, A., 2016. Managing agricultural phosphorus to minimize water quality impacts.
722 *Scientia Agricola 73*(1), 1-8. DOI Link: http://dx.doi.org/10.1590/0103-9016-2015-0107
723
724 Søvik, A.K. and Kløve, B., 2005. Phosphorus retention processes in shell sand filter systems
725 treating municipal wastewater. *Ecol. Eng. 25*(2), 168-182. DOI Link:
726 https://doi.org/10.1016/j.ecoleng.2005.04.007
727
728 Stumm, W., 1992. *Chemistry of the solid-water interface: processes at the mineral-water and*
729 *particle-water interface in natural systems*. John Wiley & Son Inc..
730
731 Sukačová, K., Trtílek, M. and Rataj, T., 2015. Phosphorus removal using a microalgal
732 biofilm in a new biofilm photobioreactor for tertiary wastewater treatment. *Water Res. 71*,
733 55-63. DOI Link: https://doi.org/10.1016/j.watres.2014.12.049
734
735 Tejedor-Tejedor, M.I. and Anderson, M.A., 1990. The protonation of phosphate on the
736 surface of goethite as studied by CIR-FTIR and electrophoretic mobility. *Langmuir 6*(3), 602-
737 611. DOI Link: http://doi.org/ 0743-7463/90/ 2406-0602$02.50/0
738
739 Tresintsi, S., Simeonidis, K., Katsikini, M., Paloura, E.C., Bantsis, G. and Mitrakas, M.,
740 2014. A novel approach for arsenic adsorbents regeneration using MgO. *J. Hazard. Mater.*
741 *265*, 217-225. DOI Link: https://doi.org/10.1016/j.jhazmat.2013.12.003

Ujaczki, É., Feigl, V., Molnár, M., Cusack, P., Curtin, T., Courtney, R., O'Donoghue, L., Davris, P., Hugi, C., Evangelou, M.W. and Balomenos, E., (2018). Re-using bauxite residues: benefits beyond (critical raw) material recovery. *Journal of Chemical Technology & Biotechnology* 93(9), 2498-510. DOI Link: https://doi.org/10.1002/jctb.5687

United Nations. 2015. Transforming our world: the 2030 agenda for sustainable development. Available: http://www.un.org/en/development/desa/population/migration/generalassembly/docs/globalcompact/A_RES_70_1_E.pdf [accessed 18.07.2018].

Vuković, G.D., Marinković, A.D., Škapin, S.D., Ristić, M.Đ., Aleksić, R., Perić-Grujić, A.A. and Uskoković, P.S., 2011. Removal of lead from water by amino modified multi-walled carbon nanotubes. *Chem. Eng. J. 173*(3), 855-865. DOI Link: https://doi.org/10.1016/j.cej.2011.08.036

Wang, X.X., Wu, Y.H., Zhang, T.Y., Xu, X.Q., Dao, G.H. and Hu, H.Y., 2016. Simultaneous nitrogen, phosphorous, and hardness removal from reverse osmosis concentrate by microalgae cultivation. *Water Res. 94*, 215-224. DOI Link: https://doi.org/10.1016/j.watres.2016.02.062

Weissert, C. and Kehr, J., 2018. Macronutrient sensing and signaling in plants. In *Plant Macronutrient Use Efficiency* (45-64). DOI Link: https://doi.org/10.1016/B978-0-12-811308-0.00003-X

767 Wu, K., Chen, Y., Ouyang, Y., Lei, H. and Liu, T., 2018. Adsorptive removal of fluoride
768 from water by granular zirconium–aluminum hybrid adsorbent: performance and
769 mechanisms. *Environ. Sci. Pollution Res.* 25(16),15390-403. DOI Link:
770 https://doi.org/10.1007/s11356-018-1711-1
771
772 Ye, J., Zhang, P., Hoffmann, E., Zeng, G., Tang, Y., Dresely, J., Liu, Y., 2014. Comparison
773 of response surface methodology and artificial neural network in optimization and prediction
774 of acid activation of Bauxsol for phosphorus adsorption. *Water, Air, Soil Pollut.* 225(12),
775 2225. DOI Link: https://doi.org/10.1007/s11270-014-2225-1
776
777 Zhou, Z., Hu, D., Ren, W., Zhao, Y., Jiang, L.M. and Wang, L., 2015. Effect of humic
778 substances on phosphorus removal by struvite precipitation. *Chemosphere 141*, 94-99. DOI
779 Link: https://doi.org/10.1016/j.chemosphere.2015.06.089
780
781 Zhou, B., Xu, Y., Vogt, R.D., Lu, X., Li, X., Deng, X., Yue, A. and Zhu, L., 2016. Effects of
782 land use change on phosphorus levels in surface waters—a case study of a watershed strongly
783 influenced by agriculture. *Water, Air, Soil Pollut. 227*(5), 160. DOI Link:
784 https://doi.org/10.1007/s11270-016-2855-6
785
786 Zhu, F., Li, Y., Xue, S., Hartley, W. and Wu, H., 2016. Effects of iron-aluminium oxides and
787 organic carbon on aggregate stability of bauxite residues. *Environ. Sci. Pollution Res. 23*(9),
788 9073-9081. DOI Link: https://doi.org/10.1007/s11356-016-6172-9
789

Zhu, X., Li, W., Zhang, Q., Zhang, C. and Chen, L., 2018. Separation characteristics of vanadium from leach liquor of red mud by ion exchange with different resins. *Hydrometallurgy 176*, 42-48. DOI Link: https://doi.org/10.1016/j.hydromet.2018.01.009

Table 1 Phosphorus (P) adsorption studies that have been carried out using bauxite residue, untreated and treated residues, and their recovery efficiencies (adapted from Cusack *et al.,* 2018).

	P recovery technique	Factors investigated	Type of water	Initial P concentration of the water	P recovered	Reference
Untreated bauxite residue	Batch adsorption experiment	Kinetics, pH and temperature	Synthetic water	5-100 mg P L^{-1}	0.20 mg P g^{-1}	Grace *et al.,* 2015
Untreated bauxite residue	Column study	Initial concentration, particle size	Synthetic water	60-1000 mg P L^{-1}	25 mg P g^{-1*}	Herron *et al.,* 2016
Untreated bauxite residue	Batch adsorption experiment	Initial concentration, pH, particle size	Synthetic water	10-150 mg P L^{-1}	0.345-1 mg P g^{-1}	Cusack *et al.,* 2018
Gypsum Treated	Batch adsorption experiment	Contact time	Synthetic water	20-400 mg P L^{-1}	7.03 mg P g^{-1}	Lopez *et al.,* 1998
Gypsum Treated	Batch adsorption experiment	Initial concentration, pH, particle size	Synthetic water	10-150 mg P L^{-1}	1.39-2.73 mg P g^{-1}	Cusack *et al.,* 2018
Seawater Treated	Batch adsorption experiment	Initial concentration, pH, particle size	Synthetic water	10-150 mg P L^{-1}	0.48-1.92 mg P g^{-1}	Cusack *et al.,* 2018
Brine treated bauxite residue (Bauxsol™)**	Batch adsorption experiment	pH, ionic strength, time	Synthetic water	0.5-2 mg P L^{-1}	6.5-14.9 mg P g^{-1}	Akhurst *et al.,* 2006
Brine treated bauxite residue (Bauxsol™)**	Column study	Kinetics, particle size	Secondary treated effluent	3-9.2 mg P L^{-1}	2.85-8.74 mg P g^{-1}	Despland *et al.,* 2011
Acid and brine treated bauxite residue (Bauxsol™)**	Batch adsorption experiment	Kinetics and isotherms	Synthetic water	200 mg P L^{-1}	55.72 mg P g^{-1}	Ye *et al.,* 2014
Heat treated bauxite residue	Batch adsorption experiment	Time, pH and initial concentration	Synthetic water	155 mg P L^{-1}	155.2 mg P g^{-1}	Liu *et al.,* 2007
Acid and heat treated bauxite residue	Batch adsorption experiment	Time, pH and initial concentration	Synthetic water	155 mg P L^{-1}	202.9 mg P g^{-1}	Liu *et al.,* 2007
Acid treated bauxite residue	Batch adsorption experiment	Acid type, pH	Synthetic water	1 mg P L^{-1}	1.1 mg P g^{-1}	Huang *et al.,* 2008

*P_{max} value given i.e. Maximum amount of P adsorbed per g of media, as determined using the Langmuir adsorption isotherm.

**Bauxsol™ = neutralised bauxite residue produced using the Basecon™ procedure, which uses brines high in Ca^{2+} and Mg^{2+} (McConchie *et al.,* 2001).

821 **Table 2** Main mineralogical composition (%) of the bauxite residue determined by XRF.

Mineral oxide	%
Aluminum oxide, Al_2O_3	14.8 ± 1.5
Iron oxide, Fe_2O	47.5 ± 2.0
Titanium oxide, TiO_2	10.3 ± 0.95
Silicon oxide, SiO_2	7.20 ± 1.0
Calcium oxide, CaO	6.1 ± 1.0

822

823 **Table 3** Particle size distribution of the bauxite residue used in this study.

d_{10} (µm)[a]	d_{50} (µm)[b]	d_{90} (µm)[c]
0.8 ± 0.1	2.6 ± 0.1	6.8 ± 0.2

824 [a]d_{10} (µm) = the size of particles at 10% of the total particle distribution.
825 [b]d_{50} (µm) = the median; the size of particles at 50% of the total particle distribution.
826 [c]d_{90} (µm) = the size of particles at 90% of the total particle distribution.
827

828

829

830

831

832

833

834

835

836

837

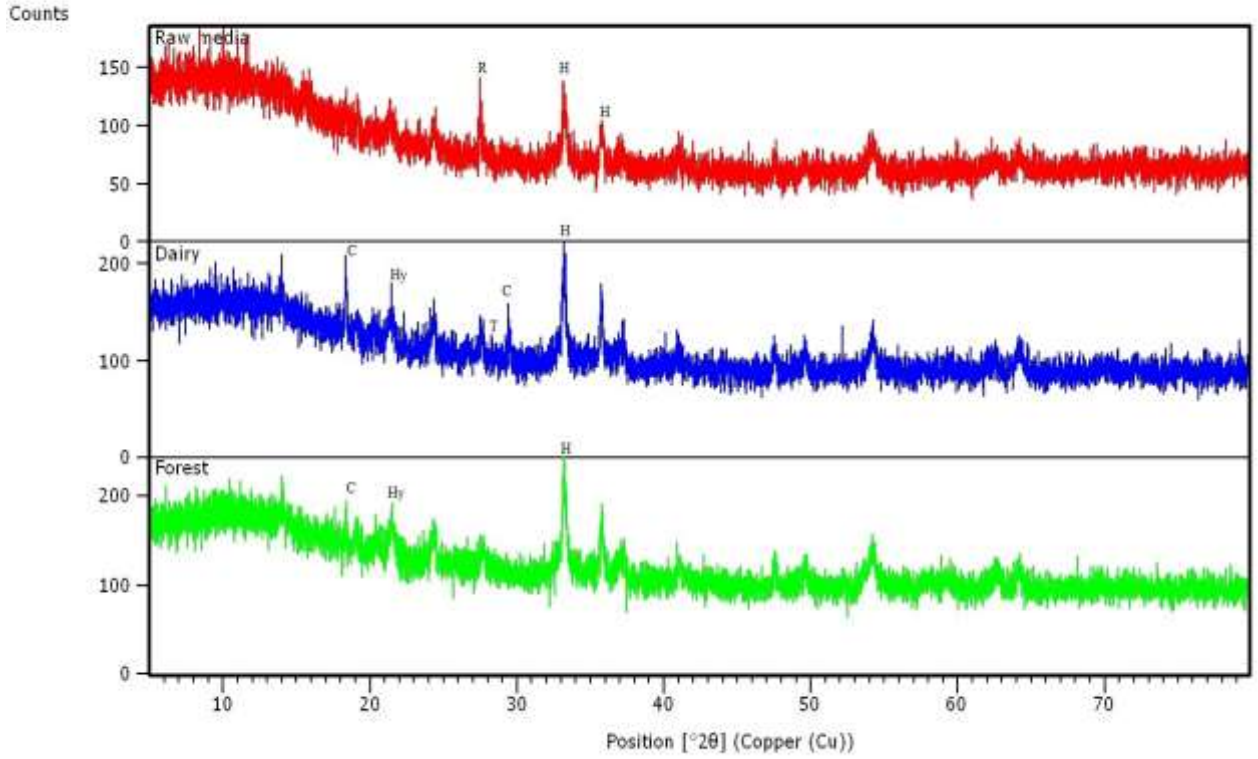

838 **Figure 1** XRD pattern as determined for the column media before ('Raw media', top) and after the
839 loading period with DSW ('Dairy', middle) and forest run-off ('Forest', bottom). Hematite (H;
840 Fe_2O_3), detected at position 33.153 and 35.612°2Θ and rutile (R; TiO_2), detected at position 27.459
841 °2Θ were present in the raw bauxite residue media. Calcium hydrogenphosphate (III) hydrate (C;
842 $CaHPO_4^{3-}$), detected at positions 19.120 and 30.001 °2Θ, was present in both the spent media
843 following treatment of the DSW and forest run-off.
844
845
846
847

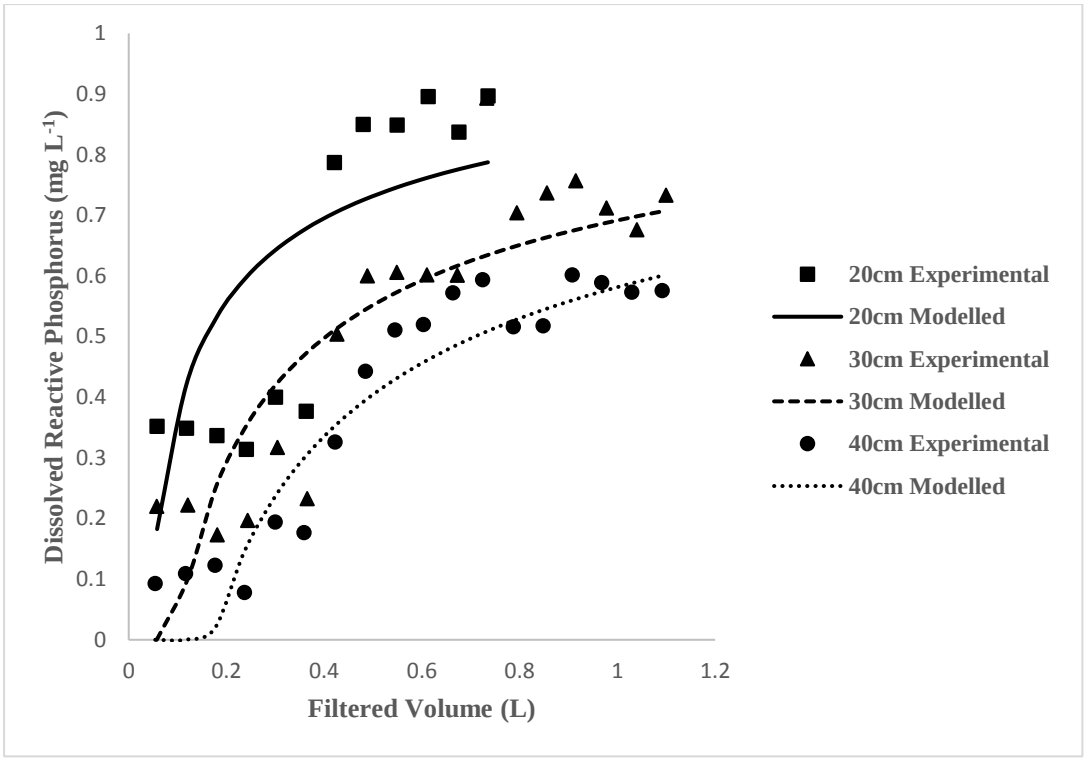

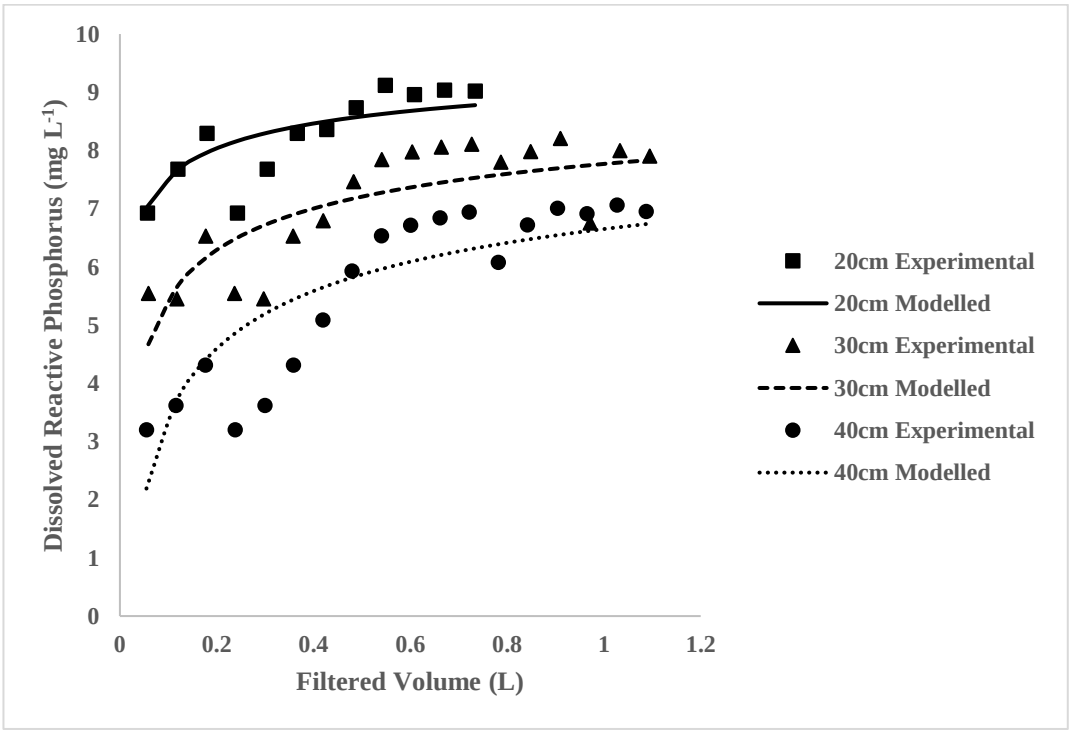

Figure 2 The breakthrough curves for the effluent dissolved reactive phosphorus concentration versus loading time for forest run-off (top) and dairy soiled water (bottom) using experimental and modelled data.

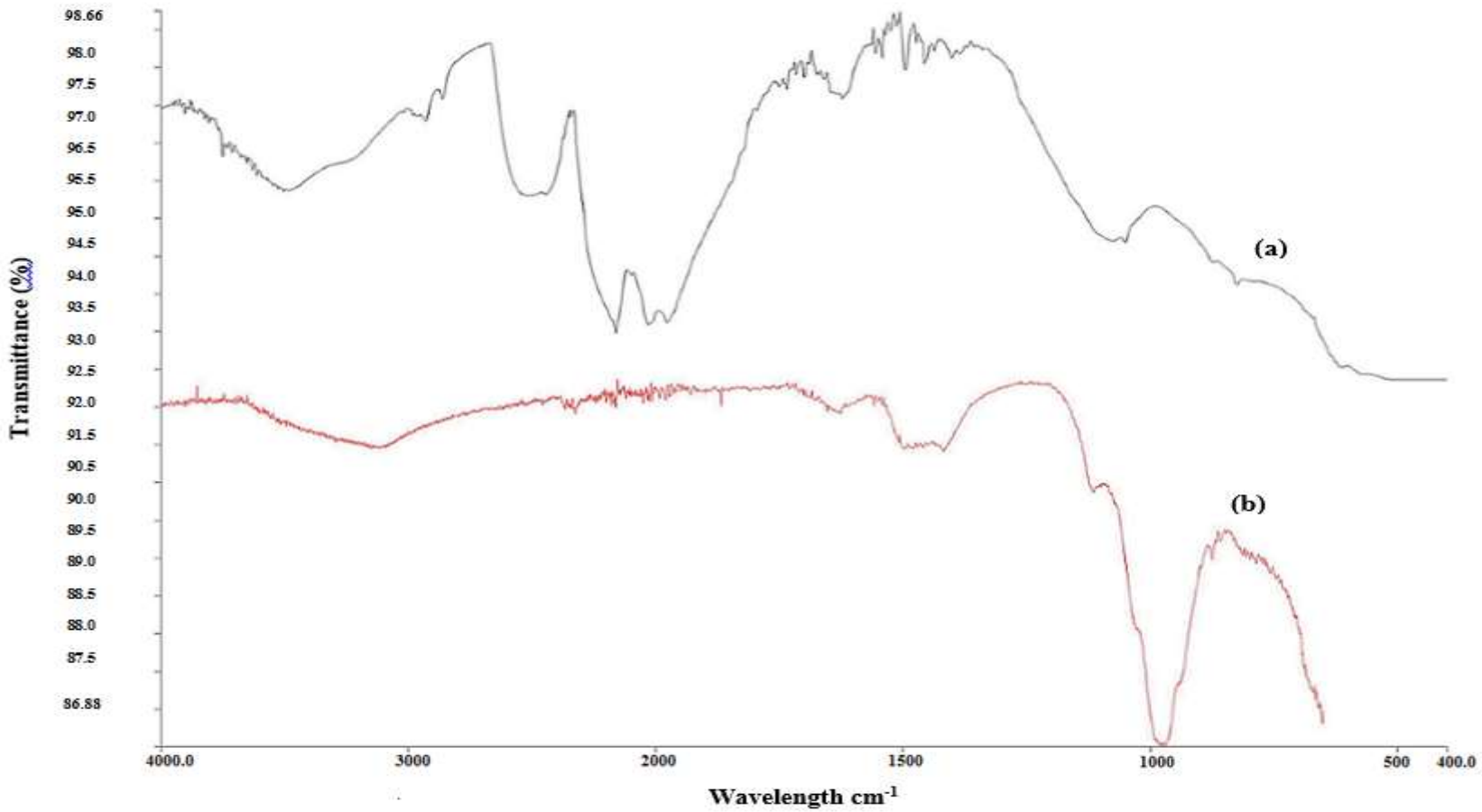

852 **Figure 3** FT-IR analysis of the bauxite residue media before (a) and after use in the column treating DSW (b).

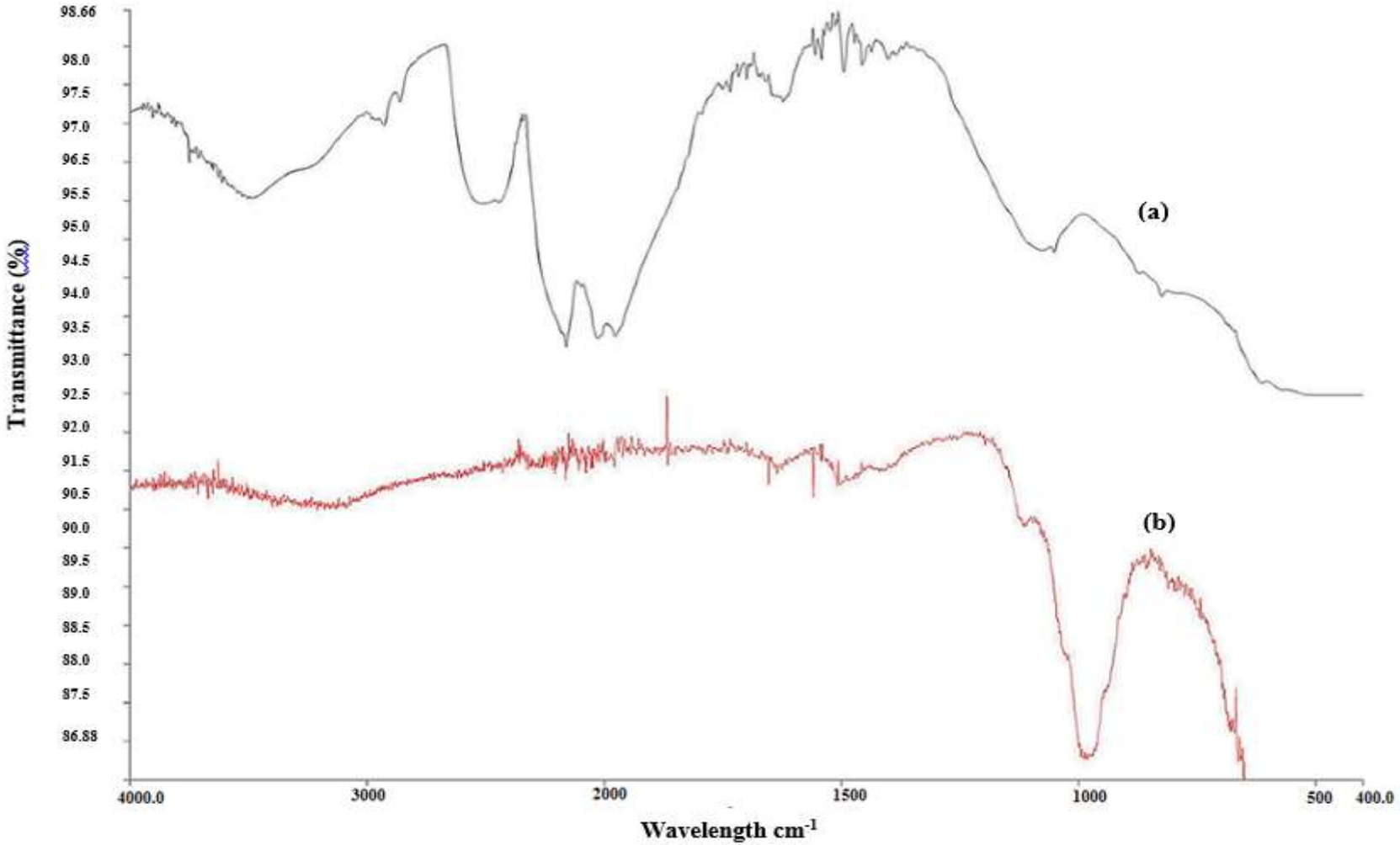

853 **Figure 4** FT-IR analysis of the bauxite residue media before (a) and after use in the column treating forest run-off (b).

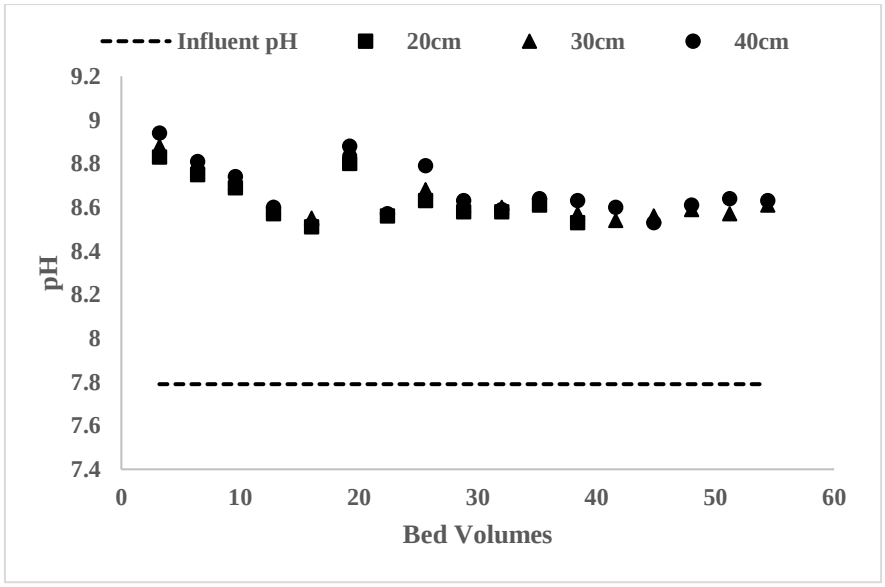

(a)

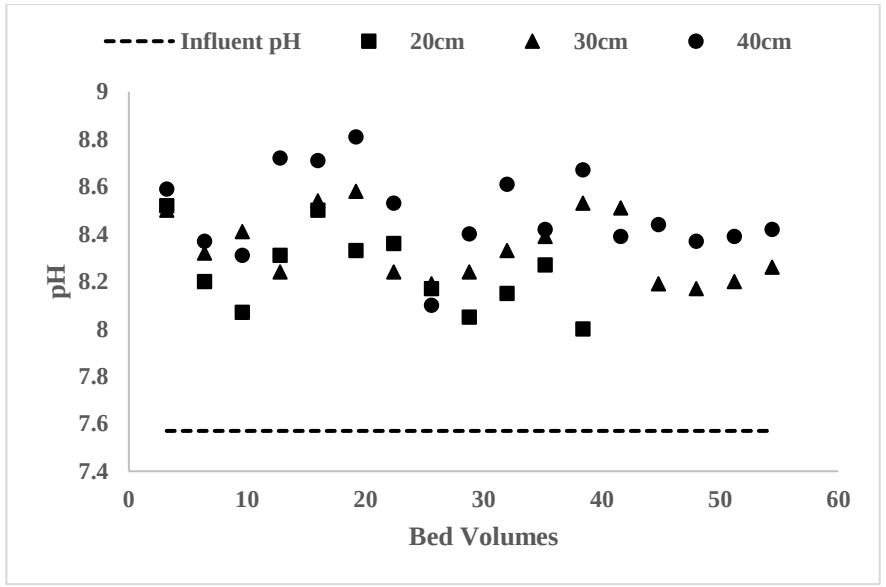

(b)

854 **Figure 5** The pH values of (a) the dairy soiled water and (b) forest run-off effluent from the columns over the 24 – 36 hr loading period, showing that there

855 was an overall increase in the pH of the effluent treated.

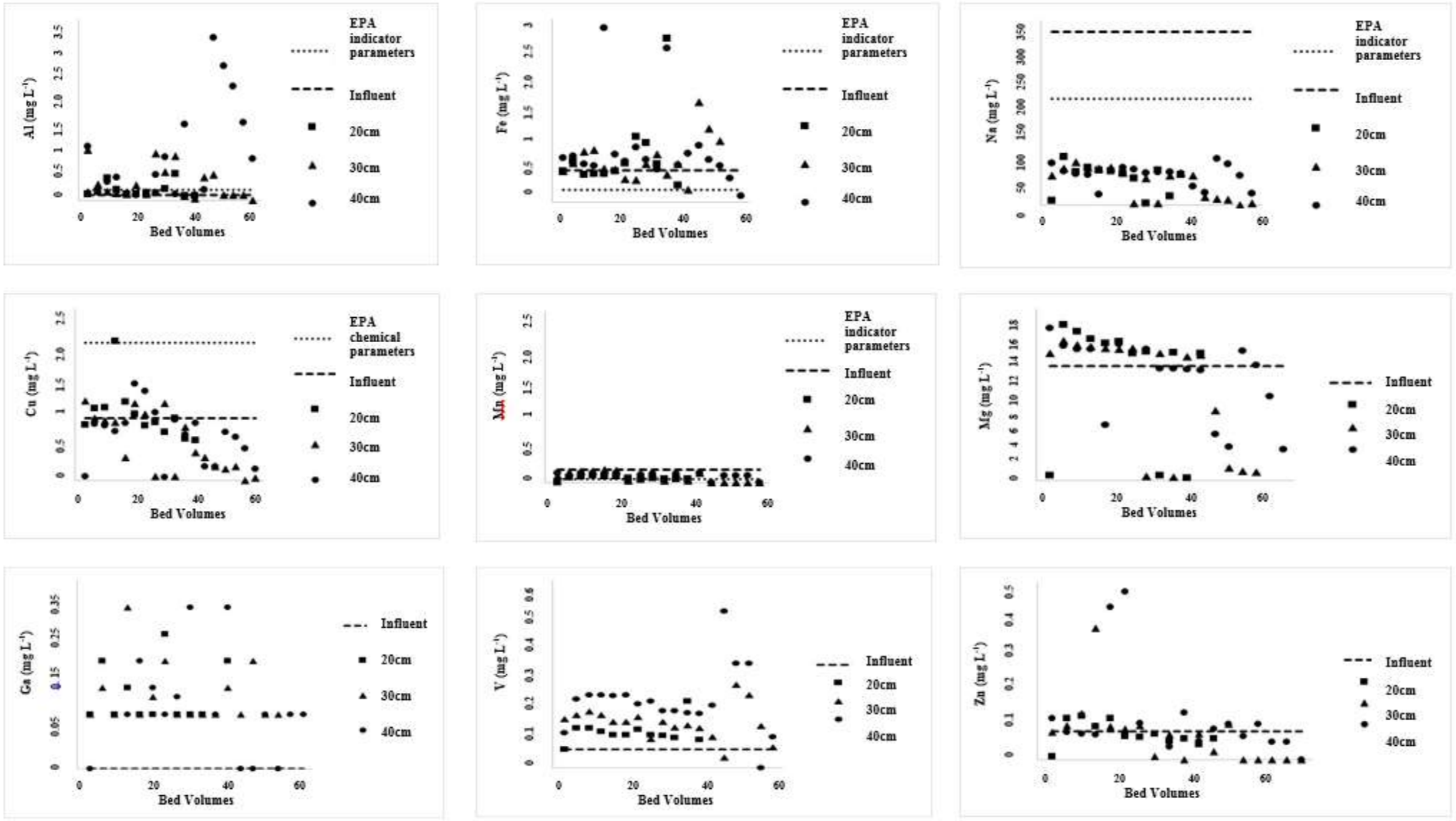

Figure 6 Comparison of the composition of (a) Al, (b) Fe, (c) Na (d) Cu (e) Mn (f) Mg (g) Ga (h) V and (i) Zn in both the influent and effluent in the columns treating DSW over the 24 -36 hr loading period. EPA indicator parameter or EPA chemical parameter included for each element.

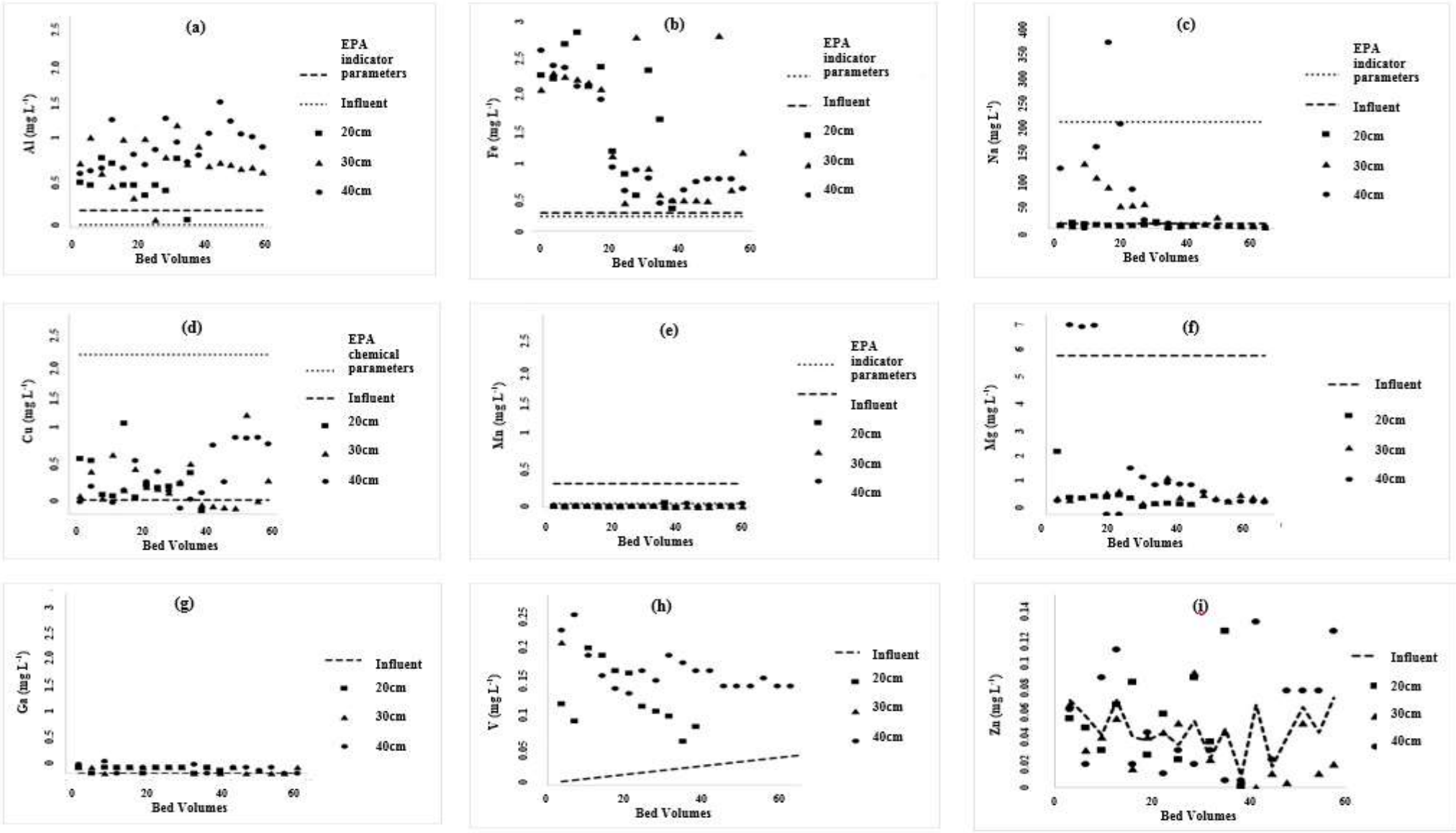

Figure 7 Comparison of the composition of (a) Al, (b) Fe, (c) Na (d) Cu (e) Mn (f) Mg (g) Ga (h) V and (i) Zn in both the influent and effluent in the columns treating forest run-off over the 24 -36 hr loading period. EPA indicator parameter or EPA chemical parameter included for each element.

862

863